Modeling of a Simplified Indirect Pumped Thermal Energy Storage System

To

Professor Greg Nellis

ME 491

Mitchell Haglund | mjhaglund@wisc.edu

Mechanical Engineering Department | University of Wisconsin-Madison

December 22, 2021

Introduction

Issues in Electricity Production and Intermittent Renewable Energy Sources

In 2019, fossil fuels generated 16,144 TWh of electricity, meaning about 12 percent of total fossil fuel consumption was devoted to producing electricity [1]. Alternative energy sources for electricity like nuclear and renewables have made significant headway in recent years, but fossil fuels still produce about two-thirds of all electricity worldwide [1]. Electricity demand will only increase as electricity takes over sectors historically driven by fossil fuels, including the transportation sector, where the popularity of electric vehicles has exploded in the past decade [2]. This presents a difficult paradox, because even as such sectors nominally move away from fossil fuels and towards electricity, their dependence on fossil fuels remains intact.

However, owing to recent progress in alternative energy solutions, the electricity sector has excellent potential for rapid, large-scale emission reductions. Renewable energy sources (RESs), the most common of which are wind and solar, show promise as sustainable and scalable alternatives to fossil fuels. Currently, they account for only 10 percent of all electricity production [3]. Cost is one reason for this diminutive stake; in most cases, RESs are more expensive per unit of energy produced than fossil fuels. That said, the gap is rapidly shrinking. Figure 1 shows the levelized cost of energy (LCOE) for wind and solar energy since 2010.

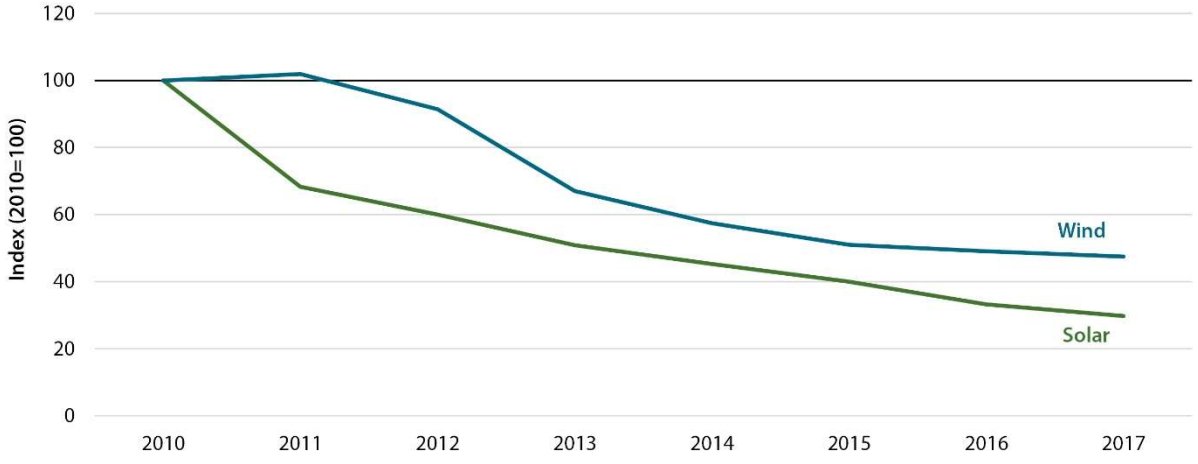

Figure 1. Levelized cost of energy (LCOE) for solar and wind [4]. LCOE is a common unitless measure of energy production that normalizes the cost relative to some specified amount. Here, the 2010 cost is set to 100, thus in 2017, solar energy was 30 percent as expensive per unit of energy as in 2010, for example.

Furthermore, when considering the economic burdens of fossil fuels in climate change effects, RESs are far cheaper [4].

As costs become more palatable for consumers, some RESs like wind and solar still face another obstacle: intermittency. With solar, for example, when the sun is shining with little interference, solar farms may produce more power than their local demand and waste the excess energy. This phenomenon is called "curtailment," which represents a critical source of inefficiency in intermittent RESs. Furthermore, when the sun sets or passes behind a cloud, the produced power is not sufficient to meet the demand.

At its core, intermittency is a major supply and demand issue that inhibits the integration of RESs into electrical grids. The unreliable and constantly fluctuating supply from intermittent RESs leads to voltage destabilization and rapid power swings in the grid. In this way, only up to 15 percent of the power used in a given grid may come from intermittent sources [5].

Electrical energy storage solutions are necessary to solve the intermittency issue. In essence, electrical energy storage captures curtailed electricity and delivers it when generation is low. Figure 2 demonstrates this for solar energy by overlaying demand (load), solar radiation, and power delivered with 6 hours of energy storage.

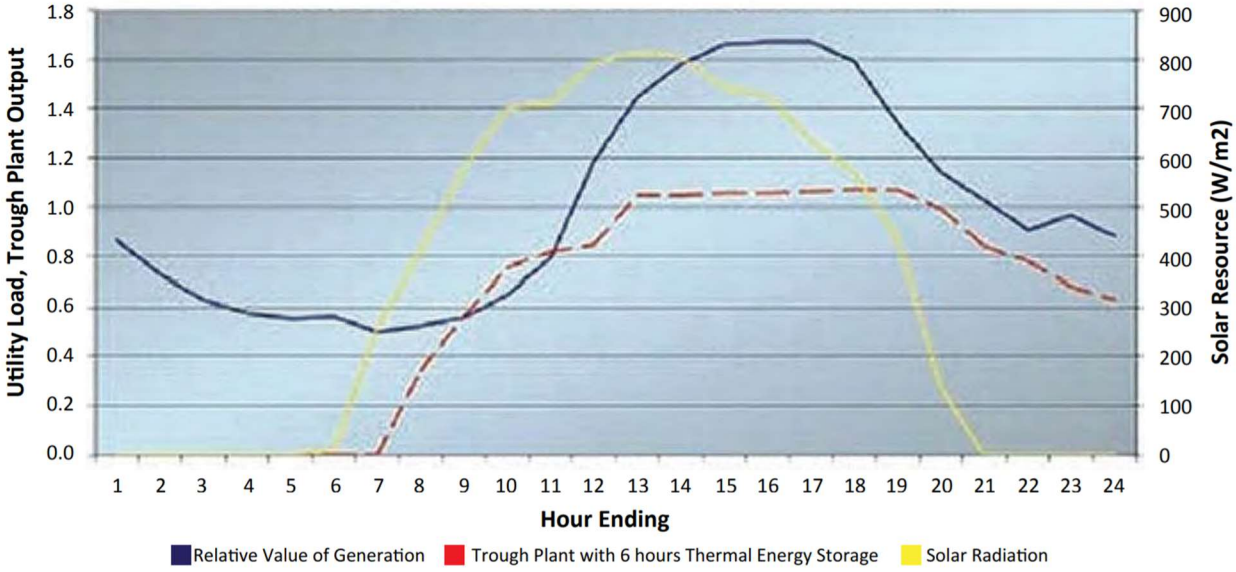

Figure 2. The effect of electrical energy storage on curtailment [6]. This plot represents data from a concentrated solar power tower with thermal energy storage. The blue line is the "Relative Value of Generation", which can be thought of as the normalized demand where 1.0 is the average.

It is clear from Figure 2 that just a few hours of storage can significantly reduce curtailment and deliver power even when the sun has long set. More storage brings greater benefits; Figure 3 shows how storage duration affects curtailment.

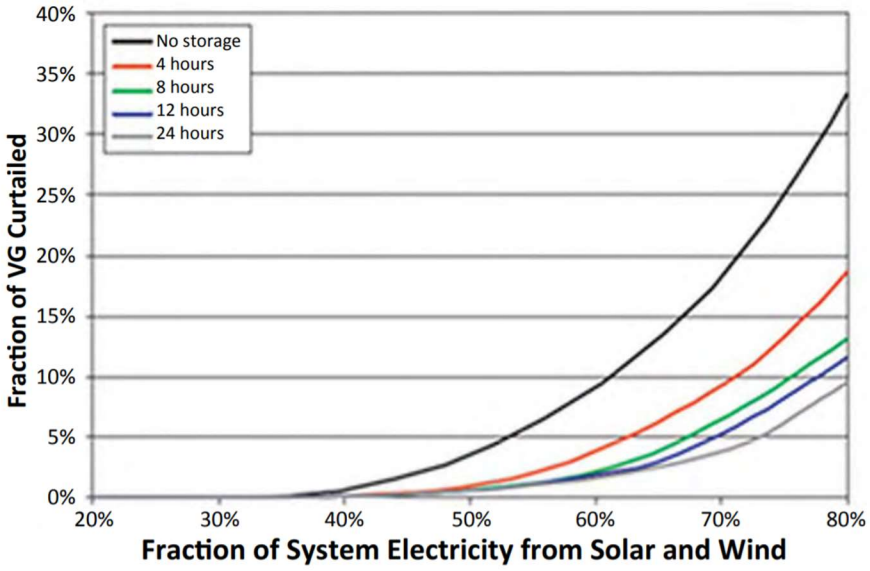

Figure 3. The effect of storage duration on curtailment [6]. VG refers to "variable generation," which is simply the power produced from intermittent sources.

More discussion of intermittency effects can be found in [5] and [6].

The flexibility and efficiency offered by energy storage is auspicious, and its development is necessary if renewables are to have a meaningful stake in electricity generation going forward. Pumped hydro storage (PHS), compressed air energy storage (CAES), and large-scale lithium ion (Li-ion) batteries are a few storage technologies currently employed. PHS is, however, by far the most common, accounting for over 90 percent of all energy stored [7]. PHS systems capture the potential energy of a water reservoir elevated relative to a second reservoir during discharge and pump the water back up while charging. PHS offers round-trip efficiencies of 65-87 percent, and its technology is well-established. However, geographic inflexibility is a major disadvantage of PHS; the location must support two large reservoirs at elevations that change rapidly. Additional disadvantages include high investment costs and extensive land requirements [8]. Given the relative popularity of PHS despite its glaring issues, storage solutions clearly require significant advancement. Further discussion of electrical energy storage can be found in [7], [8], [9], [10], and [11].

Description of Pumped Thermal Energy Storage

Pumped thermal energy storage (PTES), also called pumped heat electricity storage (PHES), is a proposed storage technology that aims to address the critical issues of current storage solutions, including high costs, geographic dependence, and low energy density. This section describes proposed PTES designs and how they work, an experimental PTES build, and potential advantages and disadvantages relative to current storage technologies.

Operation and Proposed Designs

PTES systems leverage thermodynamic cycles to convert between electricity and thermal energy. Every PTES system will contain a working fluid running through a cycle containing a compressor, an expander (turbine), a hot reservoir, a cold reservoir, and at least one heat exchanger [12]. Since 2010, several PTES designs have come forth that use these elements in various configurations. Up to now, PTES designs fall into three general categories: Brayton, transcritical Rankine, and compressed heat energy PTES systems.

A schematic of a Brayton cycle developed by White [13] is given in Figure 4.

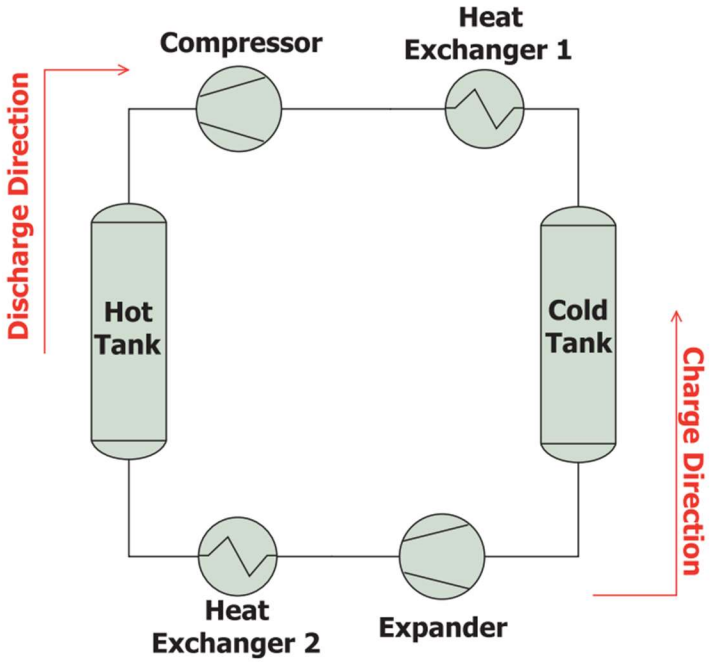

Figure 4. Simple schematic of a Brayton PTES system [12]. Arrows are given corresponding to the charge and discharge flow directions, but the turbomachinery shown is configured to the charge phase. The top compressor changes to an expander when discharging, and the bottom expander changes to a compressor.

While charging, the working fluid is in a low-pressure state before entering the compressor, adding heat and pressure to the fluid. The fluid then enters a hot reservoir containing thermal material, creating a gradient where the temperature is greater at the inlet than at the outlet. The colder fluid leaves the hot reservoir before passing through an expander, bringing the fluid back to the low-pressure state and capturing some energy. The fluid then enters the cold reservoir, again creating a temperature gradient, but here the outlet is warmer than the inlet. Finally, the fluid travels to the compressor and begins the cycle again, continually heating the hot reservoir and cooling the cold reservoir. PTES systems operate as a "heat pump" during the charge phase. During the discharge phase, the flow reverses direction, the compressor changes to an expander, the expander changes to a compressor, and energy is drawn out of the hot reservoir. Here, the cycle is working as a "heat engine." The heat exchangers shown in Figure 4 play a critical role when considering the complete

charge-discharge cycle; inefficiencies in the equipment add excess heat to the fluid, and the heat exchangers eject this excess heat to prevent system destabilization.

The working fluid in proposed Brayton PTES systems is typically air, CO2, helium, or argon [12], [14]. These systems use reservoirs with sensible heat storage, meaning that the working fluid does not change phases. This contrasts with latent heat storage, which leverages the energy generated by materials undergoing a phase change [15]. Sensible heat reservoirs are often packed beds of an inexpensive porous basalt gravel medium [12], [14], [16]. The transcritical Rankine and compressed heat energy storage PTES systems use latent storage, which inhibits their maximum power capacities. Additionally, these methods are especially immature and do not seem to show as much promise as the Brayton method at the grid scale. An excellent overview of the current state of PTES can be found in [12].

Current Implementation

The discussion of PTES has thus far relied on theoretical estimates. However, one PTES plant was built by Newcastle University in 2019 [17]. This plant is for demonstration purposes only, though it can deliver 150 kW of electricity. Figure 5 shows the thermal reservoirs of this plant.

Figure 5. Thermal reservoirs of Newcastle University's demonstration PTES plant [18]. This plant is called the National Facility for Pumped Heat Energy Storage, and it was developed by Newcastle University and the Energy Technologies Institute.

There are no readily-available studies analyzing this plant, but a round-trip efficiency of 65 percent has been reported [16]. More time and research will determine if this plant meets its longevity goals, and larger plants are required to confirm scalability estimates. However, the promise is clear, as the power capacity and efficiency of the National Facility for Pumped Heat Energy Storage meet their expected values.

Advantages

Three key advantages of PTES are low cost, high energy density, and long lifetime. The turbomachinery and heat exchangers are already well-established, inexpensive, and clean technologies. Additionally, while the only PTES plant in operation supplies a meager 150 kW, the low cost of thermal storage media renders this technology highly scalable [16]. PTES also offers good energy density, and this density paired with clean and long-lasting components allows PTES plants to impose little environmental burden.

Disadvantages

The theoretical efficiency of PTES is somewhat low, ranging from 50 to possibly 70 percent [12], [19]. Furthermore, the efficiency decreases with storage time; due to imperfect reservoir insulation, and storage duration should not exceed a few days [11]. Lastly, and most obviously, PTES is an immature technology, and its performance at large scales is ultimately uncertain.

Simplified Modeling of Indirect Pumped Thermal Energy Storage (I-PTES)

Several variations of White's basic Brayton PTES system have been proposed. One particularly recent example put forth in May 2021 by Zhang et al. [14] removes the reservoirs into separate thermal energy storage (TES) circuits, relying on additional heat exchangers to transfer the energy between the working fluid and the reservoirs (Figure 6). This is called indirect PTES (I-PTES), which contrasts with the direct PTES (D-PTES) design shown in Figure 4. In this way, the pressure in both reservoirs may be as low as ambient temperature, greatly reducing the reservoir costs. The overall energy capital cost of the I-PTES system may be up to 40 percent less than that of a D-PTES system. This cut in cost comes at a decrease in round-trip efficiency on the order of 5.87 to 12.73 percent. However, Zhang et al. estimate this penalty may be less than 5 percent with additional optimization. All told, a round-trip efficiency of 65 percent is a reasonable goal for I-PTES systems.

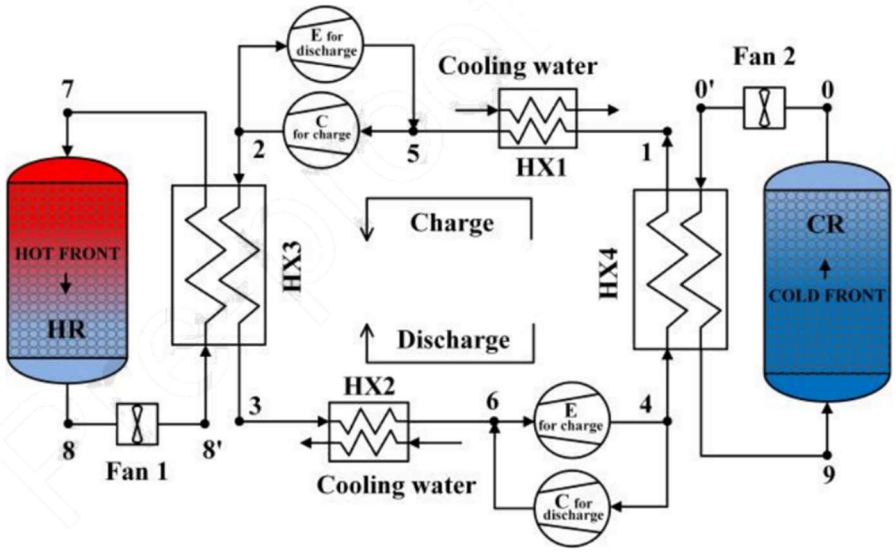

Figure 6. Schematic diagram of an I-PTES system [14].

The model used in the present report (Figure 7) is a simplified variation of the I-PTES model proposed by Zhang et al.

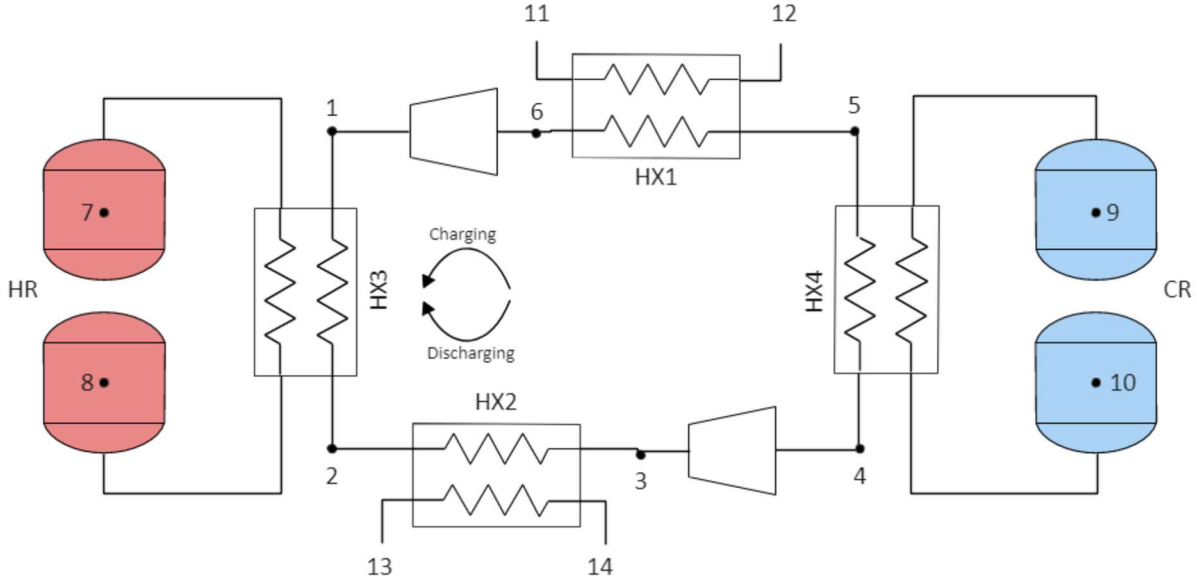

Figure 7. Schematic diagram of a simplified I-PTES system. Note that the TES circuits do not include fans, and each reservoir has two tanks filled with fluid rather than a single packed bed.

The following lists the assumptions associated with the thermodynamic analysis of the simplified I-PTES system:

- The fans in the TES circuits have very little influence on the performance of the system, thus they are omitted for simplicity.
- Transient effects of the packed-bed reservoirs are ignored. In Figure 7, the temperature gradients of the packed beds are visualized as two tanks of fluid. For example, while

charging, cold fluid at State 8 flows through HX3 and enters the tank at State 7 at a high temperature.

- Pressure drops across all heat exchangers and piping are ignored.
- The TES reservoirs are adiabatic.
- The system is operating at steady state.

Under these assumptions, three models were built in Engineering Equation Solver (EES) with different approaches to solving the system. By understanding how to leverage these models, one can easily understand and visualize how critical system parameters affect cycle performance.

EES Model Tutorials

Equipment Procedures

EES procedures are used to solve all compressor, turbine, and heat exchanger (HX) equations. The library file `HX_turbine_compressor_procedures_LIB.LIB` contains all equipment procedures. Each of the three EES models begins with a section for importing the procedure library file into the model:

```
path$ = '(local file path)…HX_turbine_compressor_procedures_LIB.LIB'
$Include path$
```

The local file path of `HX_turbine_compressor_procedures_LIB.LIB` is input as a string in the `path$` variable:

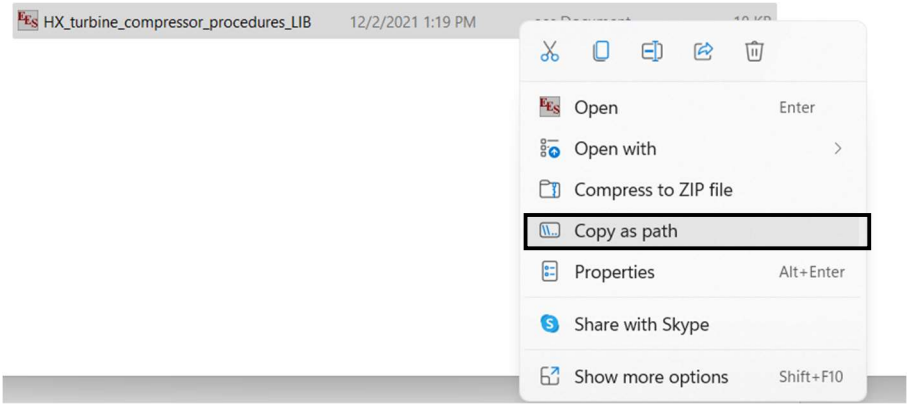

The `$Include` command then allows the procedures from the library file to be used in the model, thus avoiding some clutter in the Equations window.

Heat Exchangers

The HX procedure is called with `Call counterflow_hx(…)`. Two options are available for the HX procedure. Both options take the state parameters at the input of each fluid and the HX effectiveness to return the output state properties.

The first option leverages the energy balances shown in Equation 1,

$$\begin{aligned} \dot{q} &= \varepsilon \dot{C}_{min}\left(T_{H_{in}} - T_{C_{in}}\right) \\ &= \dot{C}_H\left(T_{H_{in}} - T_{H_{out}}\right) \\ &= \dot{C}_C\left(T_{C_{out}} - T_{C_{in}}\right) \end{aligned} \tag{1}$$

where $\dot{q}$ is the heat transfer rate between the two HX fluids, ε is the HX effectiveness, $\dot{C}$ is capacitance rate, and T is temperature. The subscripts H, C, *min*, *in*, and *out* refer to the hot fluid, cold fluid, minimum between hot and cold fluids, inlet, and outlet, respectively. The code snippet below shows the derivation of $\dot{q}$ and how it is used to generate outlet temperatures.

```
c_H = specheat(F_H$, h=h_H_in, P=P_H)          "hot fluid specific heat capacity"
c_C = specheat(F_C$, h=h_C_in, P=P_C)          "cold fluid specific heat capacity"
C_dot_H = m_dot_H*c_H                          "hot fluid capacitance rate"
C_dot_C = m_dot_C*c_C                          "cold fluid capacitance rate"
C_dot_min = min(C_dot_H, C_dot_C)              "minimum capacitance rate"
q_dot_max = C_dot_min*(T_H_in - T_C_in)        "maximum heat transfer rate between two fluids"

q_dot = eff*q_dot_max                          "actual heat transfer rate between two fluids"
T_H_out = T_H_in - q_dot/C_dot_H               "energy balance on hot fluid side"
T_C_out = q_dot/C_dot_C + T_C_in               "energy balance on cold fluid side"
```

Note that the capacitance rates are found at the inlets rather than, say, the average across the HX. This assumes the capacitance rates do not change as the fluids pass through the HX, which is not always true and may cause the HX to not balance across the full charge-discharge cycle.

The second option avoids the balancing issue by leveraging the energy balances shown in Equation 2,

$$\begin{aligned} \dot{q} &= \varepsilon \dot{q}_{max} \\ &= \dot{m}_H\left(h_{H_{in}} - h_{H_{out}}\right) \\ &= \dot{m}_C\left(h_{C_{out}} - h_{C,in}\right) \end{aligned} \tag{2}$$

where $\dot{q}$ is the heat transfer rate between the two HX fluids, ε is the HX effectiveness, $\dot{q}_{max}$ is the maximum possible heat transfer rate, $\dot{m}$ is the mass flow rate, and h is the specific enthalpy. The subscripts H, C, *in*, and *out* refer to the hot fluid, cold fluid, inlet, and outlet, respectively. The code snippet below shows the derivation of $\dot{q}$ and how it is used to generate outlet enthalpies.

```
h_2_out_max = enthalpy(F_2$, T=T_1_in, P=P_2)   "fluid 2 enthalpy if output temperature equals fluid 1 input temperature"
h_1_out_max = enthalpy(F_1$, T=T_2_in, P=P_1)   "fluid 1 enthalpy if output temperature equals fluid 2 input temperature"
q_dot_2 = m_dot_2*(h_2_out_max - h_2_in)         "energy balance if effectiveness = 1 on the fluid 2 side"
q_dot_1 = m_dot_1*(h_1_in - h_1_out_max)         "energy balance if effectiveness = 1 on the fluid 1 side"
q_dot_max = min(abs(q_dot_1), abs(q_dot_2)) "heat transfer rate if effectiveness = 1"
If (q_dot_1 < 0) Then                          "if fluid 1 is the cold fluid (NOT the assumed hot fluid)..."
    q_dot = -eff*q_dot_max                     "heat transfer rate leaving fluid 1, entering fluid 2"
Else
    q_dot = eff*q_dot_max                      "heat transfer rate leaving fluid 1, entering fluid 2"
Endif

h_1_out = h_1_in - q_dot/m_dot_1               "fluid 1 output enthalpy -- energy balance on fluid 1 side"
h_2_out = q_dot/m_dot_2 + h_2_in               "fluid 2 output enthalpy -- energy balance on fluid 2 side"
```

Note that between the two HX procedures, a different nomenclature is used (hot and cold vs. 1 and 2). In both cases, the hot and cold fluid may be input interchangeably, i.e., the input "hot" fluid need not actually be the hotter fluid to return correct outputs.

The first option is more likely to converge on a solution than the second option; however, this can be detrimental to accuracy. In some test cases, the capacitance rate changed by as much as 7 percent across a HX, thus returning outputs that violate energy conservation. Still, the first option is a useful first pass to gather reasonable guess values to ultimately be used with the second option.

Compressors and Turbines

The compressor and turbine procedures are called with `Call compressor(…)` and `Call turbine(…)`, respectively. Both procedures take inlet fluid properties and the isentropic efficiency to return the outlet properties. The compressor procedure is guided by the energy balances in Equation 3,

$$\begin{aligned} \dot{W}_c &= \frac{\dot{m}\left(h_{out,s} - h_{in}\right)}{\eta_c} \\ &= \dot{m}(h_{out} - h_{in}) \end{aligned} \tag{3}$$

where $\dot{W}_c$ is the work input to the compressor, $\dot{m}$ is the mass flow rate, h is the specific enthalpy, and η_c is the isentropic efficiency. The term $h_{out,s}$ refers to the specific enthalpy assuming an isentropic compression. The turbine procedure, represented by Equation 4, is very similar to the compressor procedure,

$$\begin{aligned} \dot{W}_t &= \eta_t \dot{m}\left(h_{in} - h_{out,s}\right) \\ &= \dot{m}(h_{in} - h_{out}) \end{aligned} \tag{4}$$

where $\dot{W}_c$ is the power output by the turbine, and η_t is the isentropic turbine efficiency.

Consistent Elements Across All Models

Diagram Window

To quickly modify system parameters and visualize the system response in a more intuitive, organized manner, each model leverages a diagram containing all key inputs and outputs. These diagrams can be accessed and edited through the EES Diagram window tool. The online EES manual [20] and this video [21] are helpful tools for modifying the Diagram window. Figure 8 shows the diagram for Model 2.

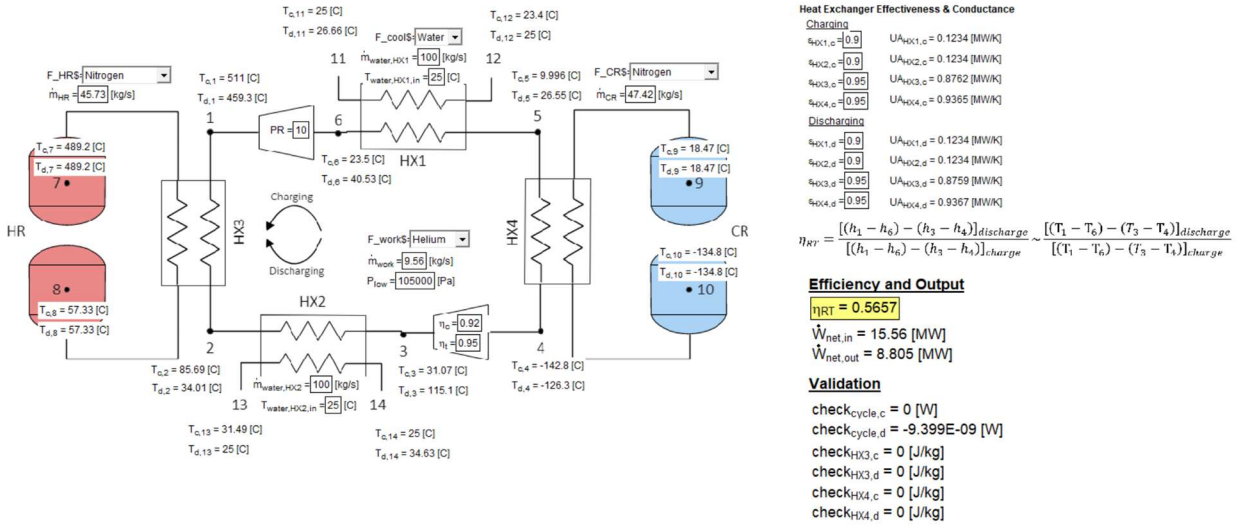

Figure 8. Diagram for Model 2. Note that each model's Diagram window contains a few different inputs and outputs.

The inputs for each model with short descriptions are provided in the Equations window immediately following the procedure import. Note that variables defined in the Equations window must not be inputs in the Diagram window and vice versa.

Equation Organization

The Equations window for each model follows the same general structure outlined below:

1. Operating conditions
2. Component performance parameters
3. State pressures
4. Solving the system
   4.1. Charging compressor/discharging turbine
   4.2. HX3
   4.3. HX2
   4.4. Charging turbine/discharging compressor
   4.5. HX4
   4.6. HX1
5. **Validation**
6. **Specific heat capacity**
7. **Capacitance rate**
8. **HX conductances**
9. Cycle performance

Note that the bolded sections do not appear in the Model 1 Equations window, as these sections are included in the Model 1 macro code.

Validation

Checks are included in each model to ensure that both the entire system and each HX is balancing energy. An energy balance across the entire system leads to Equation 5,

$$check_{cycle} = \dot{q}_{16} + \dot{q}_{HX3} + \dot{q}_{HX2} + \dot{q}_{34} + \dot{q}_{HX4} + \dot{q}_{HX1} \quad (5)$$

where $check_{cycle}$ is the sum of the energy leaving the system, $\dot{q}_{16}$ is the energy input to the compressor/turbine between states 1 and 6, $\dot{q}_{HX3}$ is the energy transferred from the hot TES circuit to the working fluid, $\dot{q}_{HX}$ is the energy transferred from the HX2 water to the working fluid, $\dot{q}_{34}$ is the energy input to the compressor/turbine between states 3 and 4, $\dot{q}_{HX4}$ is the energy transferred from the cold TES circuit to the working fluid, and $\dot{q}_{HX1}$ is the energy transferred from the HX1 water to the working fluid. All energy transfers on the right side of Equation 5 are assumed to be inputs, and the system is running at steady state, thus $check_{cycle}$ should equal 0 in a balanced system. For each model, this check is performed for the charge and discharge phases with the results shown in the Diagram window.

Equation 6 shows the energy balance check for a HX,

$$check_{HX} = (h_{in} - h_{out})_{charging} - (h_{out} - h_{in})_{discharging} \quad (5)$$

where h_{in} is the specific enthalpy entering the HX and h_{out} is the specific enthalpy leaving the same side of the HX. This check is applied to HX3 and HX4 on the working fluid side. At a given HX, the energy leaving the working fluid while charging should equal the energy entering the working fluid while discharging or vice versa. If this is true, $check_{HX}$ equals 0.

Heat Exchanger Conductance

All three models use the $\varepsilon - NTU$ method for converting HX effectiveness to conductance. EES offers a built-in function to retrieve *NTU* from ε, shown in Equation 6,

```
NTU=HX('counterflow', eff, C_dot_1, C_dot_2, 'NTU')
```
(6)

where eff is the effectiveness (ε), C_dot_1 is the capacitance rate on one side of the HX, and C_dot_2 is the capacitance rate on the other side of the HX. Equation 7 shows the relationship between *NTU* and conductance (*UA*),

$$NTU = \frac{UA}{\dot{C}_{min}} \tag{7}$$

where $\dot{C}_{min}$ is the minimum capacitance rate between C_dot_1 and C_dot_2.

All HXs are effectiveness-based in Model 1 and Model 2. Here, C_dot_1 and C_dot_2 are the average capacitance rates across either side of the HX. HX3 and HX4 in Model 3 are also effectiveness-based. However, HX1 and HX2 in Model 3 are approach temperature difference-based, where one side is assumed to be a reservoir, so a different approach is required. The Model 3 Equations window begins with a function definition for approachtoconductance(…). This function takes the working fluid properties as through HX1 or HX2 and returns an approximate HX conductance. First, the effectiveness is found by comparing the heat transfer rate if the approach temperature difference is zero to the actual heat transfer rate. This effectiveness is plugged into Equation 6, where C_dot_1 is the average conductance of the working fluid and C_dot_2 is 100 times greater than C_dot_1, as only the working fluid should undergo a temperature change. The factor of 100 was chosen mostly arbitrarily; it needs to be large enough to make the reservoir temperature change negligible.

Model 1: Separated Phases, Effectiveness-Based Heat Exchangers

Model 1 (**PTES_indirect_effectivness_macro.EES**) allows the charge and discharge phases to be solved individually. The alternation between charging and discharging may be performed manually or automatically with a macro. Both the manual and automatic methods are described after the Equations window walkthrough below.

Equations Window Walkthrough

"! Number of runs"
Specify how many full charge-discharge cycles are to be run in the macro.

"! Operating conditions, commented parameters are inputs in the Diagram window"
Specify all operating conditions. All commented definitions are provided in the Diagram window except for the mode$ variable, which is either manually set or set in the macro.

"! Component performance parameters, commented parameters are inputs in the Diagram window"
Specify turbomachinery efficiencies and HX effectiveness values.

"! State pressures"
Specify pressures at all states.

"! Charging compressor/discharging turbine"
If the system is charging, call the compressor(…) procedure to solve for State 1.
If the system is discharging, call the turbine(…) procedure to solve for State 6.

"! HX3"
If the system is charging, specify the State 8 (bottom hot reservoir) properties. Note that T[8] is set differently when solving manually or automatically. Call the counterflow_hx(…) procedure to solve for State 2 and State 7.
If the system is discharging, specify the State 7 (top hot reservoir) properties. Note that T[7] is set differently when solving manually or automatically. Call the counterflow_hx(…) procedure to solve for State 1 and State 8.

"! HX2"
If the system is charging, specify the State 14 (water cooling) properties. Call the counterflow_hx(…) procedure to solve for State 3 and State 13.
If the system is discharging, specify the State 13 (water cooling) properties. Call the counterflow_hx(…) procedure to solve for State 2 and State 14.

"! Charging turbine/discharging compressor"
If the system is charging, call the turbine(…) procedure to solve for State 4.
If the system is discharging, call the compressor(…) procedure to solve for State 3.

"! HX4"
If the system is charging, specify the State 9 (top cold reservoir) properties. Note that T[9] is set differently when solving manually or automatically. Call the counterflow_hx(…) procedure to solve for State 5 and State 10.

If the system is discharging, specify the State 10 (bottom cold reservoir) properties. Note that T[10] is set differently when solving manually or automatically. Call the counterflow_hx(…) procedure to solve for State 4 and State 9.

"! HX1"
If the system is charging, specify the State 11 (water cooling) properties. Call the counterflow_hx(…) procedure to solve for State 6 and State 12.
If the system is discharging, specify the State 12 (water cooling) properties. Call the counterflow_hx(…) procedure to solve for State 5 and State 11.

"! Cycle performance"
If the system is charging, the flow passes through a compressor from State 6 to State 1, and the flow passes through a turbine from State 4 to State 3.
If the system is discharging, the flow passes through a compressor from State 4 to State 3, and the flow passes through a turbine from State 1 to State 6.

Manual Operation

Before attempting to solve the system manually, ensure that the following equations are uncommented:

```
mode$ = …       "set mode 'charging' or 'discharging' "
T[8] = …        “state 8 temperature, uncomment to solve without macro”
T[7] = …        “state 7 temperature, uncomment to solve without macro”
T[9] = …        “state 9 temperature, uncomment to solve without macro”
T[10] = …       “state 10 temperature, uncomment to solve without macro”
```

Note that these equations are highlighted blue in the Equations window. The following will describe an example how these above equations are modified during manual operation.

T_HR and T_CR are set in the Diagram window. T_HR and T_CR are the initial temperatures corresponding to State 8 (lower hot reservoir) and State 9 (upper cold reservoir), respectively. In this example, T_HR is set to 50 °C and T_CR is set to 20 °C. These are functionally guess values, and the reservoir temperatures will change with each subsequent run until converging on a constant solution.

Next, mode$ is set to 'charging', T[8] is set to T_HR, and T[9] is set to T_CR:

```
mode$ = 'charging'      "set mode 'charging' or 'discharging' "
T[8] = T_HR             “state 8 temperature, uncomment to solve without macro”
T[9] = T_CR             “state 7 temperature, uncomment to solve without macro”
```

Solve the Equations window. Note that the Diagram window will not provide any useful information, however the Arrays Table will contain the relevant properties for all 14 states. During

the charging process, HX3 heats the 50 °C State 8 fluid before entering the State 7 tank. During discharge, this hot State 7 fluid is cooled by HX3 before entering the State 8 reservoir. The process is similar on the cold reservoir side. Therefore, to model the discharge, mode$ is set to 'discharging' while T[7] and T[10] are set to their corresponding values in the Arrays Table:

Set T[7] to this value →

Set T[10] to this value →

Arrays Table

Main

Sort	1 T_i [K] {[C]}	2 s_i [J/kg-K]	3 P_i [Pa]	4 h_i [J/kg]
[1]	784.6 {511.5}	28146	1.050E+06	4.083E+06
[2]	352.2 {79.05}	23987	1.050E+06	1.838E+06
[3]	303.6 {30.4}	23215	1.050E+06	1.585E+06
[4]	130 {-143.1}	23594	105000	680763
[5]	284.6 {11.45}	27662	105000	1.483E+06
[6]	296.8 {23.69}	27881	105000	1.547E+06
[7]	762.5 {489.3}	7821	105000	804688
[8]	323.2 {50}	6909	105000	335297
[9]	293.2 {20}	6807	105000	304053
[10]	138.1 {-135}	6021	105000	142228
[11]	298.2 {25.05}	367.9	105000	105133
[12]	296.7 {23.6}	347.5	105000	99055
[13]	303.9 {30.78}	447.4	105000	129075
[14]	298.2 {25}	367.2	105000	104924

```
mode$ = 'discharging'              "set mode 'charging' or 'discharging'
T[7] = converttemp(C,K,489.3)      "state 7 temperature, uncomment to solve without macro"
T[10] = converttemp(C,K,-135)      "state 10 temperature, uncomment to solve without macro"
```

Solve the Equations window. Unless the initial T_HR and T_CR guesses were precisely correct, T[8] and T[9] will be slightly different. To repeat the charge phase, set T[8] and T[9] to their corresponding array values as performed in the first discharge phase, ensuring that the mode$ variable is changed accordingly. This process is repeated to simulate consecutive charge-discharge phases.

The only useful values that manual operation will return are the temperature, specific entropy, pressure, and specific enthalpy at each state. Manual operation of Model 1 does not support calculations for round-trip efficiency, HX conductance, energy balance checks, etc. Additionally, manual operation is quite cumbersome and inefficient. However, this method is valuable for understanding how the complete PTES cycle works in a stepwise fashion. Also, manual operation is an effective way to validate that automatic operation is functioning properly.

Automatic Operation

The EES macro tool greatly expedites the process detailed in the *Manual Operation* section while also providing much more detail regarding system performance. The Macro window can be opened with CTRL+M or the icon on the toolbar shown below:

The user will be prompted to open an EES Macro File (EMF), which is **PTES_indirect_effectiveness_macro_EMF.EMF**. A snippet of the Macro window is shown below:

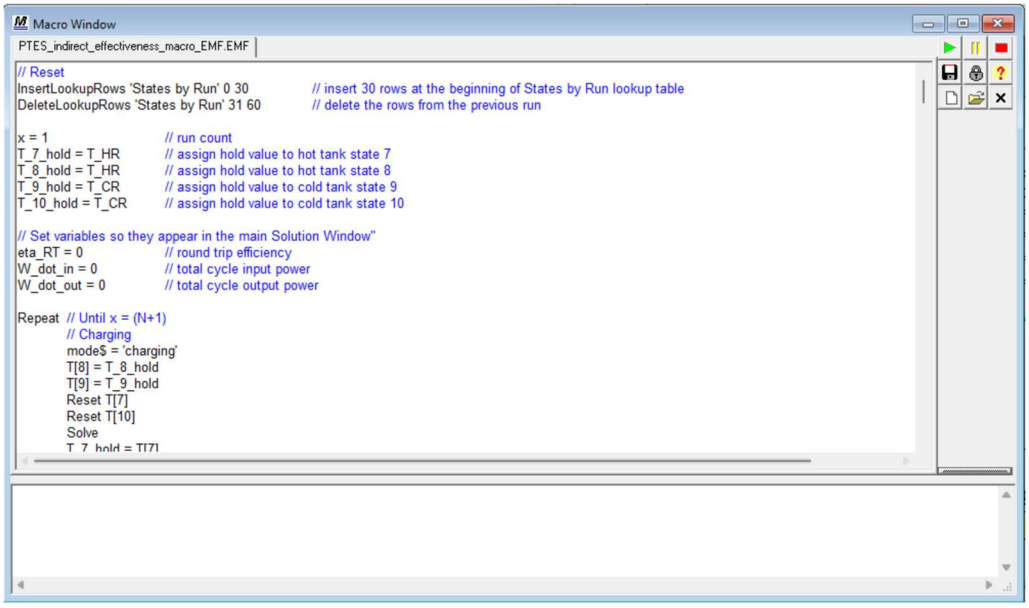

The lock icon toggles whether the code may be edited. Note that performing actions within EES, such as solving or saving, will add possibly unwanted lines of code to the macro. This can be avoided by toggling the lock icon, which greys out the code as shown below:

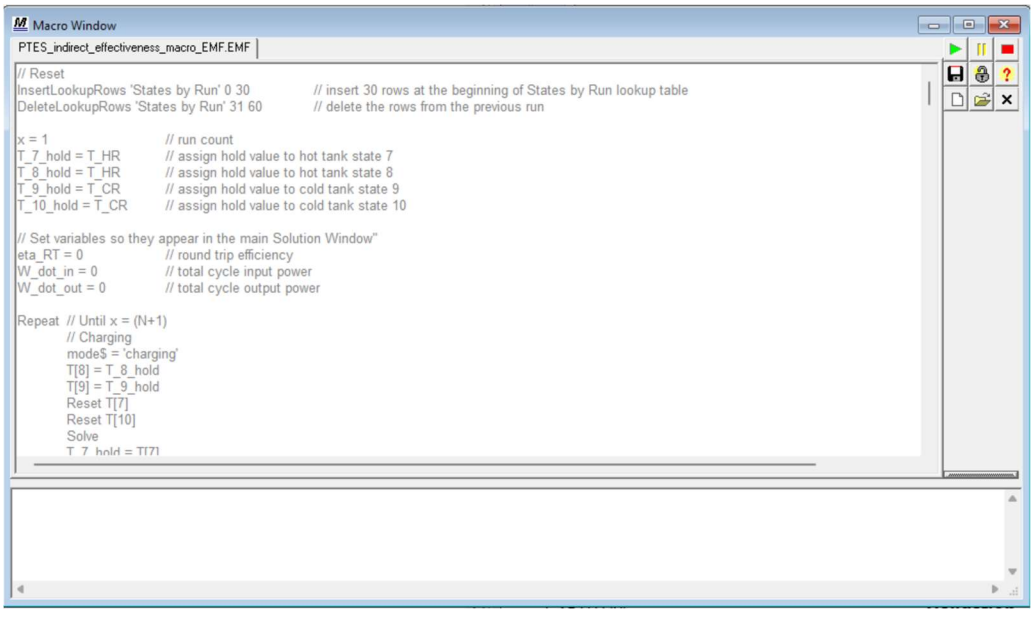

To run the macro, toggle the green play symbol in the macro or the EES toolbar. To save the macro, click the save icon in the Macro window. Note that saving the EES file does not also save the macro file.

The following walks through the macro code in a similar fashion to the *Equations Window Walkthrough*:

// Reset

Model 1 contains a Lookup table called 'States by Run' that holds a column for each state temperature in charging and discharging. For example, the State 1 charging temperature is T_table_c_1. There are 30 rows for a maximum of 30 full charge-discharge cycles per macro execution. The first two lines of code in the // Reset section insert 30 rows to the start of 'States by Run' and delete the 30 rows from the previous macro execution, effectively clearing the Lookup table.

The variable x represents the current run count, which starts at 1.

As discussed in the *Manual Operation* section, depending on whether the system is charging or discharging, a reservoir may end one phase and begin the next at the same temperature. The _hold values account for this. For now, they are set to T_HR or T_CR.

// Set variables so they appear in the main Solution Window"

For unknown reasons, variables defined in the loops later in the code do not appear in the Solutions window. One workaround is to define these variables with dummy values before entering the loop.

Repeat

Begin a loop until x equals one more than the desired run count N.

> // Charging
>
> Carry out the same steps described in the *Manual Operation* section for the charging cycle. First, mode$ is set to 'charging'. Then, T[8] and T[9] are set to hold temperatures, which, for the first run, is T_HR and T_CR, respectively. These hold temperatures are updated after every discharge phase.
>
> Solve the Equations window, and the hold values for T[7] and T[10] are updated to their corresponding array values.
>
> W_dot_in is the total power input to the system while charging. This is used later to calculate the round-trip efficiency of the current run.
>
> // Populate lookup table 'States by Run' with state temperatures for the current run (charging)
>
> Add temperatures at each state to 'States by Run' during the charge phase for the current run. For example, when Lookup['States by Run', x, 'T_table_c_1'] = T[1] is executed and x equals 2 (second run), the first column and second row is populated with the temperature at charge State 1.
>
> // Discharging

This section is functionally identical to // Charging, but in reverse. Here, W_dot_out is the total power output from the system while discharging. Again, this is used later to calculate the round-trip efficiency of the current run.

// Populate lookup table 'States by Run' with state temperatures for the current run (discharging)
This section functions the same as // Populate lookup table… (charging), but now populating the discharge phase columns.

If (x < N) then GOTO 1 // in the final run, perform the following block
Execute the following code block on the very last run (x = N). If it is not the final run, skip the following code block and continue at Label 1: // Resume code here if x < N. All outputs displayed in the Diagram window are from the final run.

> // Charging state temperature from the last row in the 'States by Run' lookup table; displayed in the Diagram Window
> // Discharging state temperature from the last row in the 'States by Run' lookup table; displayed in the Diagram Window
>
> These two sections assign the values in the last row of 'States by Run' to their final array temperatures. For example, T_c[1] and T_d[1] are the final run State 1 temperatures for charging and discharging, respectively.
>
> // Charging state pressure (could be done at any point in the previous code)
> // Discharging state pressure (could be done at any point in the previous code)
> // Charging state specific enthalpy
> // Discharging state specific enthalpy
> // Charging state specific entropy
> // Discharging state specific entropy
> // Charging state specific heat capacity
> // Discharging state specific heat capacity
> // Charging state capacitance rate
> // Discharging state capacitance rate
> Assign all the relevant properties for each state to the Arrays Table.
>
> //Validation
> Perform the energy balance checks described in *Consistent Elements Across all Models: Validation*.
>
> //Heat exchanger conductances; displayed in the Diagram Window
> Perform HX conductance calculations described in *Consistent Elements Across all Models: Heat Exchanger Conductance.*

Label 1: // Resume code here if x < N
Resume code from this point if the current run is not the final run.
Record the round-trip efficiency and run count for the current run.

Update x for next run. This is equivalent to x = x+1 in other programming languages like Python.

Until x = (N+1)
Close loop when the run count has reached the specified value N.
Collect the round-trip efficiency for the final run.

Discussion

Model 1 is an excellent tool for understanding how the system operates and how individual parameters influence system performance. One can observe charge-discharge cycles representing "fake" solutions, i.e., systems that would destabilize with subsequent cycle runs. For example, if HX1 and HX2 are removed while retaining imperfect turbomachinery efficiencies, Models 2 & 3 would not converge on a solution. Through the "States by Run" Lookup table and Figure 1-4 in the Plots window, one can observe why the system destabilizes. *System Analyses: Heat Exchanger Effects* includes further discussion of this topic.

Model 2: Combined Phases, Effectiveness-Based Heat Exchangers

Model 2 (**PTES_indirect_effectivness.EES**) solves the charging and discharge phases simultaneously. Each HX is effectiveness-based such that no states can be explicitly defined. The reservoir states 7, 8, 9, and 10 stay constant between charging and discharging, which constrain the complete charge-discharge cycle. This model is much less complex and computationally expensive than Model 1, as the Equations window only needs to be solved once to converge on a solution.

Equations Window Walkthrough

"! Operating conditions, commented parameters are inputs in the Diagram window"
Specify all operating conditions. All commented definitions are provided in the Diagram window.

"! Component performance parameters, commented parameters are inputs in the Diagram window"
Specify turbomachinery efficiencies and HX effectiveness values.

"! State pressures"
Specify pressures at all states.

"! Charging compressor/discharging turbine"
Call the compressor(…) procedure to solve for charging State 1.
Call the turbine(…) procedure to solve for discharging State 6.

"! HX3"

"Charging"
The State 8 (lower hot reservoir) temperature stays the same between charging and discharging. Specify the remaining charging State 8 properties. Call the counterflow_hx(…) procedure to solve for charging State 2 and State 7.
"Discharging"
The State 7 (upper hot reservoir) temperature stays the same between charging and discharging. Specify the remaining discharging State 7 properties. Call the counterflow_hx(…) procedure to solve for discharging State 1 and State 8.

"! HX2"
"Charging"
Specify State 14 (water cooling) properties. Call the counterflow_hx(…) procedure to solve for charging State 3 and State 13.
"Discharging"
Specify State 13 (water cooling) properties. Call the counterflow_hx(…) procedure to solve for discharging State 2 and State 14.

"! Charging turbine/discharging compressor"
Call the turbine(…) procedure to solve for charging State 1.
Call the compressor(…) procedure to solve for discharging State 6.

"! HX4"
"Charging"
The State 9 (upper cold reservoir) temperature stays the same between charging and discharging. Specify the remaining charging State 9 properties. Call the counterflow_hx(…) procedure to solve for charging State 5 and State 10.
"Discharging"
The State 10 (lower cold reservoir) temperature stays the same between charging and discharging. Specify the remaining discharging State 10 properties. Call the counterflow_hx(…) procedure to solve for discharging State 4 and State 9.

"! HX1"
"Charging"
Specify State 11 (water cooling) properties. Call the counterflow_hx(…) procedure to solve for charging State 6 and State 12.
"Discharging"
Specify State 12 (water cooling) properties. Call the counterflow_hx(…) procedure to solve for discharging State 5 and State 11.

"! Cycle performance"
If the system is charging, the flow passes through a compressor from State 6 to State 1, and the flow passes through a turbine from State 4 to State 3.
If the system is discharging, the flow passes through a compressor from State 4 to State 3, and the flow passes through a turbine from State 1 to State 6.

"! Validation"
Perform the energy balance checks described in *Consistent Elements Across all Models: Validation*.

"! Specific heat capacity"
"! Capacitance rate"
"! Heat exchanger conductances; displayed in the Diagram Window"
Perform HX conductance calculations described in *Consistent Elements Across all Models: Heat Exchanger Conductance.*

"! Cycle performance"
Calculate total input power, total output power, and round-trip efficiency.

Discussion

If convergence is possible, Model 1 and Model 2 will find to the same results given the same input parameters. Furthermore, the stepwise operation of Model 1 may provide some insight into why Model 2 may not converge under certain parameters. These two models can thus be used to check and validate one another.

The advantages of Model 2 over Model 1 are two-fold: For one, Model 2 solves much faster than Model 1, allowing the user to efficiently observe how tweaking parameters affects system performance. Secondly, Model 2 is a much better option for optimization and parametric studies; this model is used extensively in the *System Analyses* section.

Model 3: Combined Phases, Approach Temperature Difference-Based Heat Exchangers

Model 3 (**PTES_indirect_approachTemps.EES**) is identical to Model 2 in all respects except for the modeling of the heat rejection HXs (HX1 & HX2). To avoid redundancy with Model 2, this section will not include an Equations window walkthrough.

The general equation for the approach temperature difference model is given by Equation 8.

$$T_{out} = T_{res} \pm \Delta T_{approach} \tag{8}$$

Here, T_{out} is the temperature of the working fluid leaving the HX, T_{res} is the reservoir temperature, and $\Delta T_{approach}$ is the approach temperature difference. The corresponding equations in Model 3 are shown below:

"! HX2"
"Charging"

```
T_c[3] = T_water_HX2_in + DELTAT_approach_HX2      "state 3 temperature -- HX2 approach temperature difference"
"Discharging"
T_d[2] = T_water_HX2_in + DELTAT_approach_HX2      "state 2 temperature -- HX2 approach temperature difference"

"! HX1"
T_c[6] = T_water_HX1_in - DELTAT_approach_HX1      "state 6 temperature -- HX1 approach temperature difference"
T_d[5] = T_water_HX1_in + DELTAT_approach_HX1      "state 5 temperature -- HX1 approach temperature difference"
```

T_water_HX2_in and T_water_HX1_in correspond to T_{res} in Equation 8. Note that the sign of the approach temperature difference (DELTAT_approach_HX1, DELTAT_approach_HX2) is situationally dependent, and the above code will not apply for every set of parameters. If the input working fluid temperature is greater than the reservoir temperature, for example, ensure that the output working fluid temperature remains greater than the reservoir temperature. The sign is subject to change as other system parameters are modified.

Discussion

The approach temperature difference modeling of HX1 and HX2 allows the system to have several explicitly defined states, allowing Model 3 to converge more readily than Model 1 or Model 2. Currently, Model 3 assumes that the approach temperature difference is the same for both the charge and discharge phases. This assumption is not possible in a practical situation unless the conductance of the heat exchanger is changed between charge and discharge, which is not reasonable. This can be corrected to some degree by implementing separate approach temperature differences for the charge and discharge phase; however, the accuracy is limited by the user's patience in tweaking these temperatures. Model 3 is best suited for rough, first-pass approximations whose outputs may be transferred as guess values to Model 1 and Model 2.

System Analysis

This section details the analyses carried out on the system described in *Introduction: Simplified Model of Indirect Pumped Thermal Energy Storage (I-PTES)*. These analyses focus on understanding the effects of component performance parameters on total system behavior. The default operating conditions and component performance parameters are given by Table 1.

Table 1. Default operating conditions and component performance parameters.

			Model		
		EES Variable	**1**	**2**	**3**
Operating Conditions	Working fluid	F_work$	Helium		
	Hot reservoir fluid	F_HR$	Nitrogen		
	Cold reservoir fluid	F_CR$	Nitrogen		
	Cooling fluid	F_cool$	Water		
	Flow rate of working fluid [kg/s]	m_dot_work	9.56		
	Flow rate of hot reservoir fluid [kg/s]	m_dot_HR	45.73		
	Flow rate of cold reservoir fluid [kg/s]	m_dot_CR	47.42		
	Flow rate of cooling fluid through HX1 [kg/s]	m_dot_water_HX1	100		-
	Flow rate of cooling fluid through HX2 [kg/s]	m_dot_water_HX2	100		-
	Initial hot reservoir temperature [°C]	T_HR	50	-	
	Initial cold reservoir temperature [°C]	T_CR	20	-	
	Temperature of cooling fluid through HX1 [°C]	T_water_HX1_in	25		-
	Temperature of cooling fluid through HX2 [°C]	T_water_HX2_in	25		-
	Low pressure in working circuit [Pa]	P_low	105000		
	Pressure of hot reservoir circuit [Pa]	P_HR	105000		
	Pressure of cold reservoir circuit [Pa]	P_CR	105000		
Component parameters	Isentropic turbine efficiency	eta_t	0.95		
	Isentropic compressor efficiency	eta_c	0.92		
	Pressure ratio	PR	10		
	Effectiveness of HX1 while charging	epsilon_HX1_c	0.9		-
	Effectiveness of HX1 while discharging	epsilon_HX1_d	0.9		-
	Effectiveness of HX2 while charging	epsilon_HX2_c	0.9		-
	Effectiveness of HX2 while discharging	epsilon_HX2_d	0.9		-
	Effectiveness of HX3 while charging	epsilon_HX3_c	0.95		
	Effectiveness of HX3 while discharging	epsilon_HX4_d	0.95		
	Effectiveness of HX4 while charging	epsilon_HX3_c	0.95		
	Effectiveness of HX4 while discharging	epsilon_HX4_d	0.95		
	HX1 approach temperature difference [K]	DELTAT_approach_HX1	-		1.5
	HX2 approach temperature difference [K]	DELTAT_approach_HX2	-		9

Patterns in Round-Trip Efficiency

The round-trip efficiency is the ratio of energy output from the system while discharging to the energy input while charging. Equation 9 shows the round-trip efficiency (η_{RT}) calculation,

$$\eta_{RT} = \frac{[(h_1 - h_6) - (h_3 - h_4)]_{discharge}}{[(h_1 - h_6) - (h_3 - h_4)]_{charge}} \sim \frac{[(T_1 - T_6) - (T_3 - T_4)]_{discharge}}{[(T_1 - T_6) - (T_3 - T_4)]_{charge}} \quad (9)$$

where h and T are the specific enthalpy and temperature, respectively, for a given state. The helium working fluid behaves like an ideal gas such that the specific enthalpy is functionally proportional to temperature.

Observing changes in the system's T-s diagram is a useful means of understanding how the system parameters affect round-trip efficiency. Figure 9 displays the T-s diagram for the I-PTES system under the default parameters listed in Table 1.

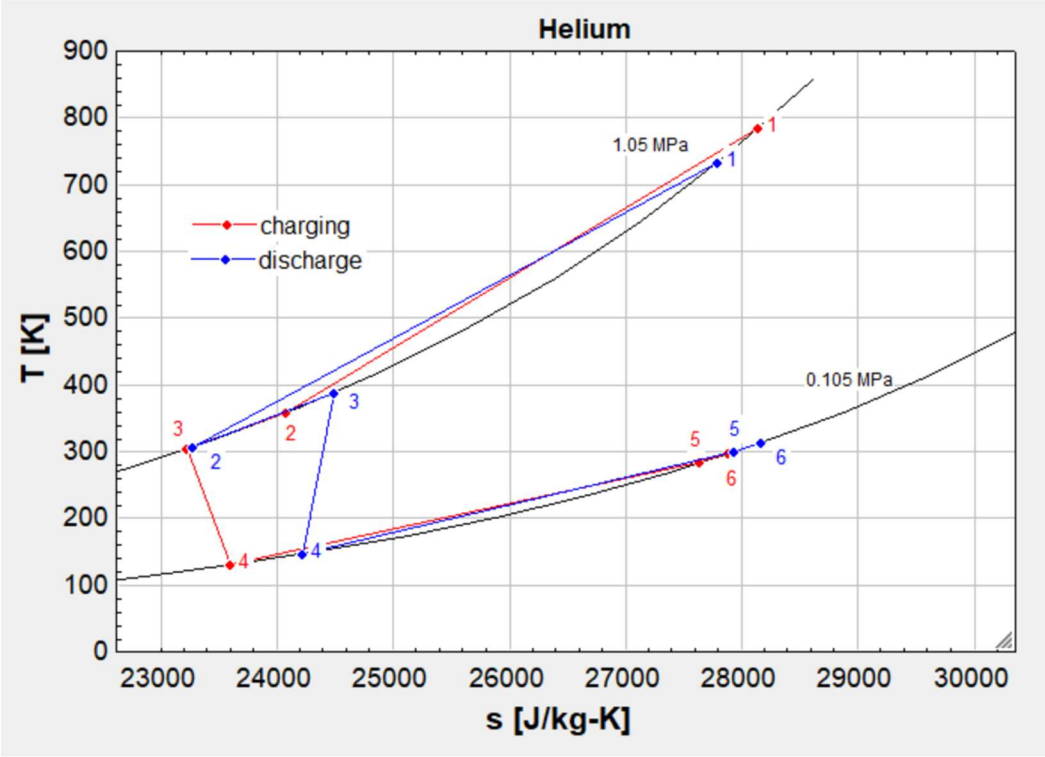

Figure 9. T-s diagram of simplified I-PTES system at default parameters (Table 1). Plot can be found as Figure 2-1 in the Model 2 Plot windows.

From Equation 9, it is clear that $(h_1 - h_6)_{discharge}$ and $(h_3 - h_4)_{cha}$ should be maximized, while $(h_3 - h_4)_{discharge}$ and $(h_1 - h_6)_{charg}$ should be minimized. States are somewhat linked between charging and discharge phases; thus, it can be difficult to increase while not also increasing $(h_3 - h_4)_{charging}$, for example. A new objective for round-trip efficiency optimization is to increase both $(h_1 - h_6)_{discharge}$ and $(h_1 - h_6)_{charging}$, while decreasing both $(h_3 - h_4)_{discharge}$ and $(h_3 - h_4)_{charg}$. This is based on a simple mathematical phenomenon demonstrated in Equation 10.

$$\eta = \frac{A_1 - B_1}{A_2 - B_2} \tag{10}$$

Here, η is efficiency, A_1, B_1, A_2, and B_2 are dimensionless numbers analogous to $(h_1 - h_6)_{discharge}$, $(h_3 - h_4)_{discharge}$, $(h_1 - h_6)_{charg}$, and $(h_3 - h_4)_{charg}$, respectively. Consider a case where $A_1 = A_2 = 100$ and $B_1 = B_2 = 50$:

$$\eta = \frac{100 - 50}{100 - 50} = 1$$

This represents a case where all components have perfect efficiencies. Now, let's introduce a perturbance such that A_1 and B_2 decrease by 10 percent, while A_2 and B_1 increase by 10 percent:

$$\eta = \frac{90 - 55}{110 - 45} = 0.54$$

This roughly represents a case where the turbomachinery components have imperfect efficiencies. The efficiency may be improved by increasing A_1 and A_2 to 200, for example, while retaining the same 10 percent perturbance:

$$\eta = \frac{180 - 55}{220 - 45} = 0.71$$

Similarly, the efficiency may be improved by lowering B_1 and B_2. In short, with a larger temperature difference between states 1 and 6, the system is less susceptible to perturbances from the $(h_3 - h_4)$ terms.

In summary, efforts to maximize round-trip efficiency should focus on minimizing $(h_1 - h_6)_{charge} - (h_1 - h_6)_{discharge}$ and $(h_3 - h_4)_{discharge} - (h_3 - h_4)_{charg}$. Additionally, the $(h_1 - h_6)$ terms should be maximized, and the $(h_3 - h_4)$ terms should be minimized. This can be visualized by pushing states 1 and 6 to the right while pushing states 3 and 4 to the left on the Figure 9 T-s diagram.

Heat Exchanger Effects

This section investigates the influence of the heat rejection HXs (HX1 and HX2) on system stability and performance. One method of visualizing the necessity of the heat rejection HXs is to build a perfect system, then add imperfect components. Figure 10 shows a system where the compressors, turbines, HX2, and HX3 are 100 percent efficient/effective. HX1 and HX2 are not active.

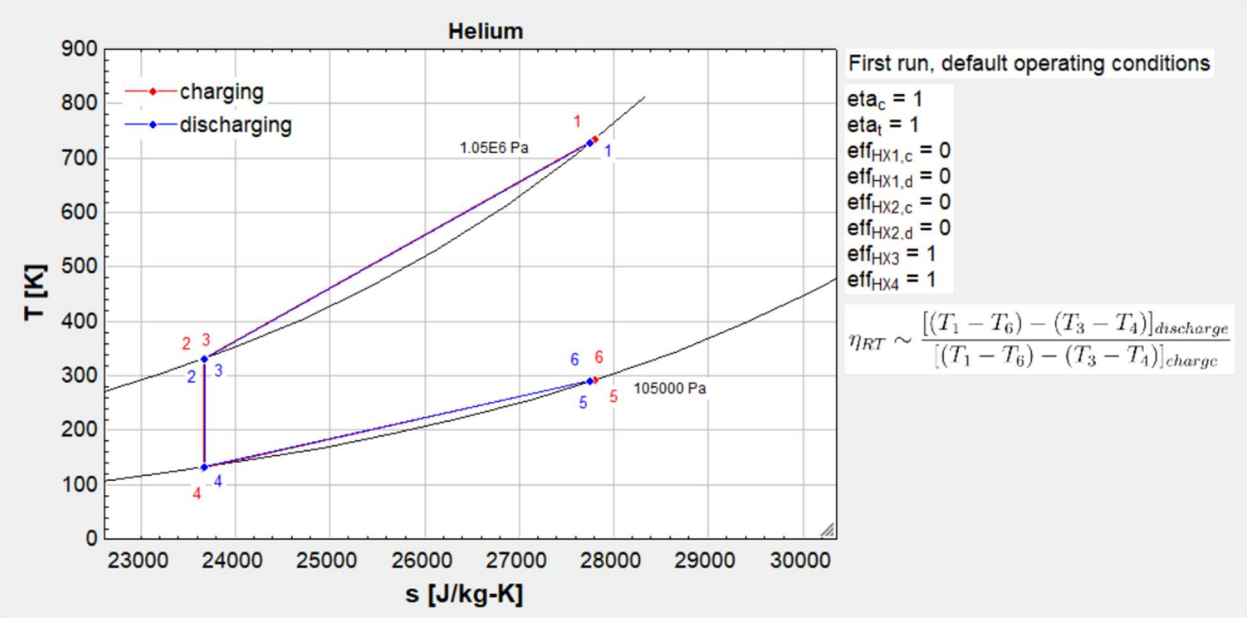

Figure 10. I-PTES cycle with perfect turbomachinery and TES HXs at default operating conditions. Plot can be found as Figure 1-1 in the Model 1 Plot windows. Note that this is only the first charge-discharge cycle to maintain stability and provide a reference for future unstable iterations.

Next, Figure 11 adds the default turbomachinery efficiencies to the system.

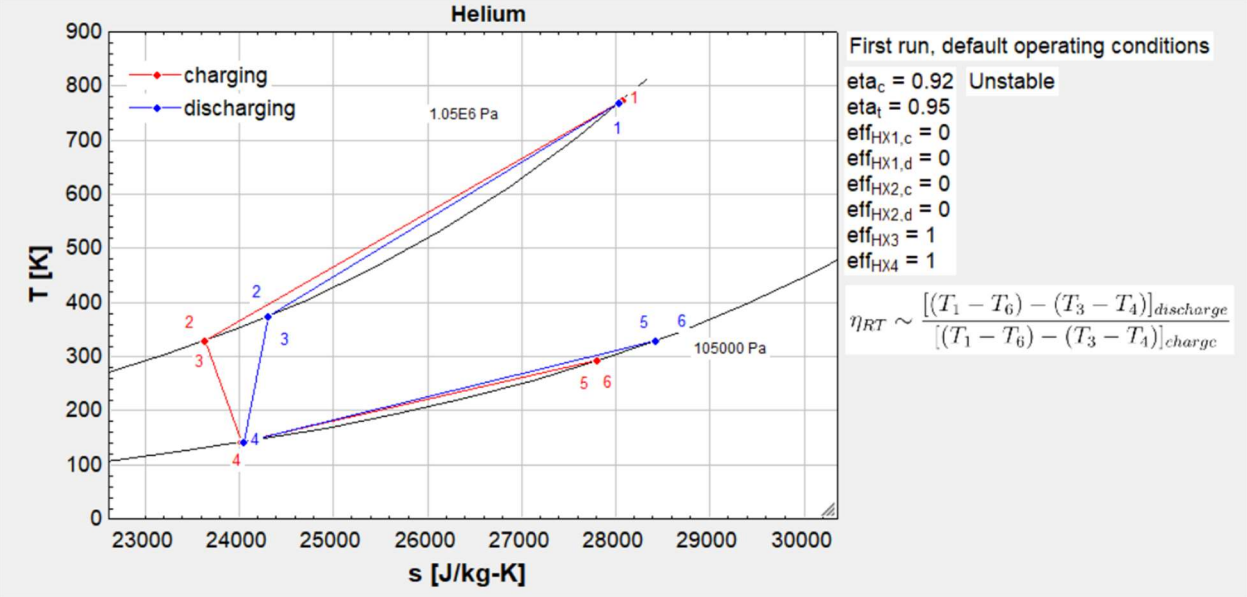

Figure 11. I-PTES cycle with default turbomachinery efficiencies and 100 percent effective TES HXs at default operating conditions. Plot can be found as Figure 1-3 in the Model 1 Plot windows. Note that this is only the first charge-discharge cycle to maintain stability and provide a reference for future unstable iterations.

Figure 11 is the first run at default operating conditions. Starting at State 1 in the charge phase, the working fluid loses heat through HX3, dropping to the default T_HR temperature at State 2/3. The fluid expands to State 4, where the entropy and temperature are higher than the isentropic

expansion shown in Figure 10. Next, the fluid is heated through HX4, climbing to the default T_CR temperature at state 5/6. The fluid is then compressed to State 1, beginning the charge phase anew. Since HX3 and HX4 are 100 percent effective, states 7 and 1 are the same temperature and states 10 and 4 are the same temperature. Therefore, the discharge State 1 temperature is approximately equal to the charge State 1 temperature. The State 1 fluid expands to State 5/6, which is hotter than the charging State 5/6. HX4 then cools the fluid to the same State 4 temperature as during the charge phase. Next, the fluid expands to State 2/3, which is hotter than the charging State 2/3, before heating back up to State 1 through HX3.

Figure 12 shows how the system continues to shift hotter on a second run.

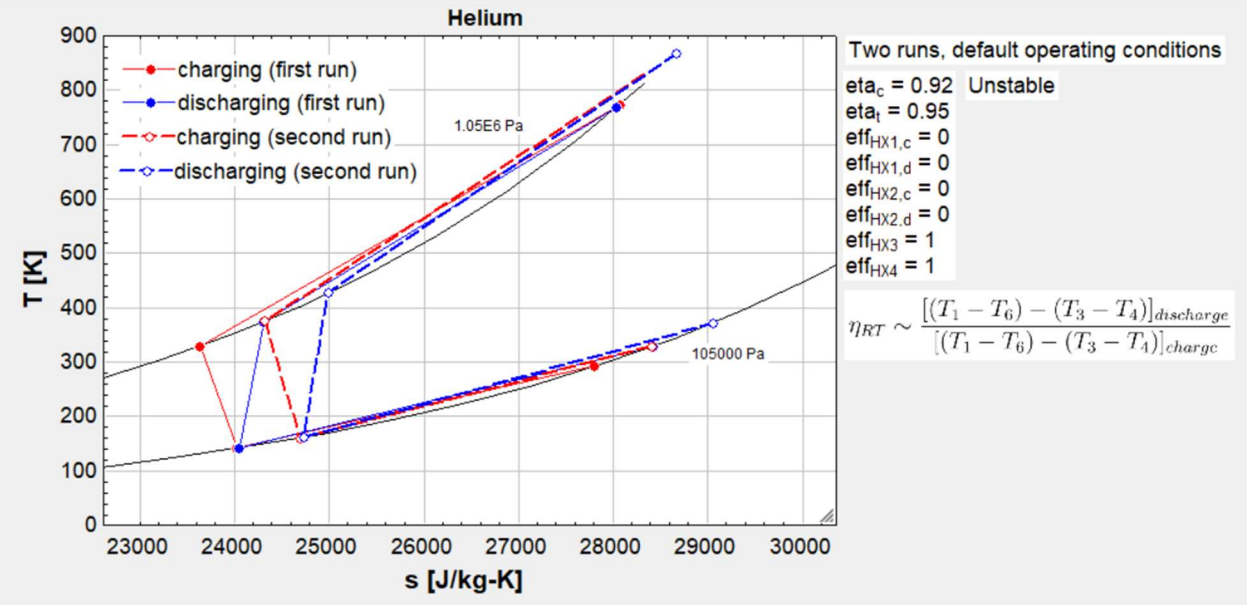

Figure 12. I-PTES cycle with default turbomachinery efficiencies and 100 percent effective TES HXs at default operating conditions; second run included to demonstrate instability. Plot can be found as Figure 1-4 in the Model 1 Plot windows.

Each subsequent charge/discharge phase builds off the last, continuously climbing in temperature and never converging. Figure 12 shows how the addition of HX1 and HX2 stabilize the system.

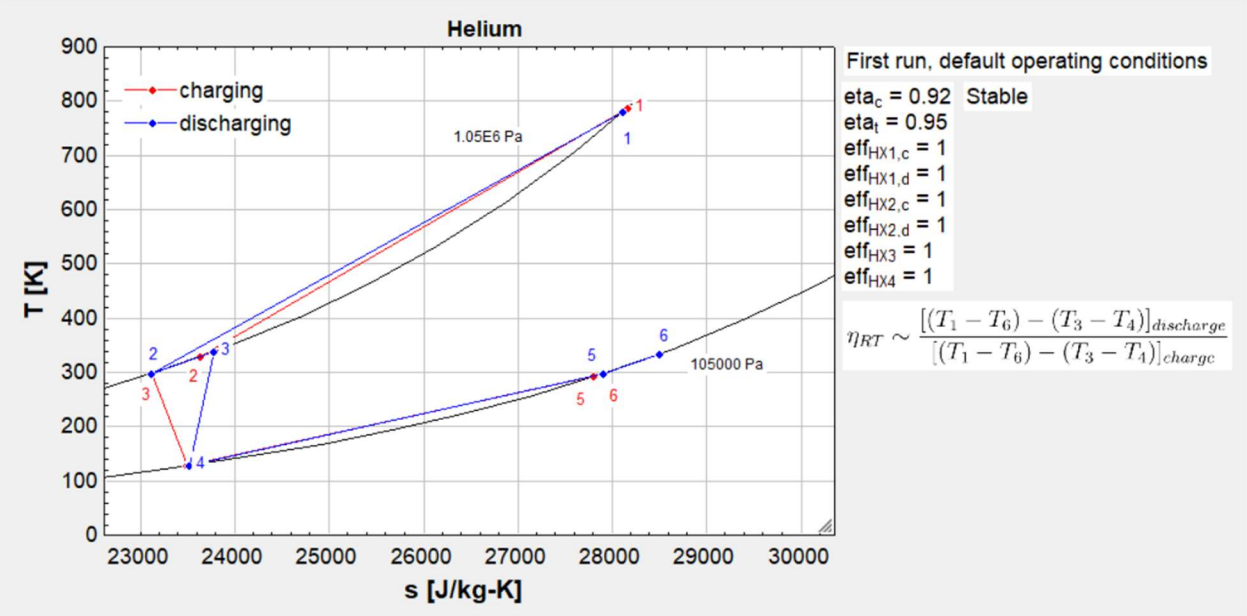

Figure 13. I-PTES cycle with default turbomachinery efficiencies and 100 percent effective HXs at default operating conditions. Plot can be found as Figure 1-6 in the Model 1 Plot windows. Note that this is only the first charge-discharge cycle.

HX1 can be thought of as pulling charge State 5 and discharge State 6 to approximately the same temperature. Similarly, HX2 pulls charge State 2 and discharge State 3 to approximately the same temperature. In this way, HX1 and HX2 prevent the "climbing" behavior shown in Figure 12. When the heat exchangers are not perfectly effective, as shown in Figure 9, this stabilizing behavior is still present given HX1 and HX2 are of sufficient effectiveness.

The principles discussed in *System Analysis: Patterns in Round-Trip Efficiency* can be utilized concerning the HX1 and HX2 water temperatures (T_water_HX1_in, T_water_HX2_in); increasing T_water_HX1_in increases the $(h_1 - h_6)$, while decreasing T_water_HX2_in decreases the $(h_3 - h_4)$ terms. Figure 14 shows the effect of water temperatures on round-trip efficiency

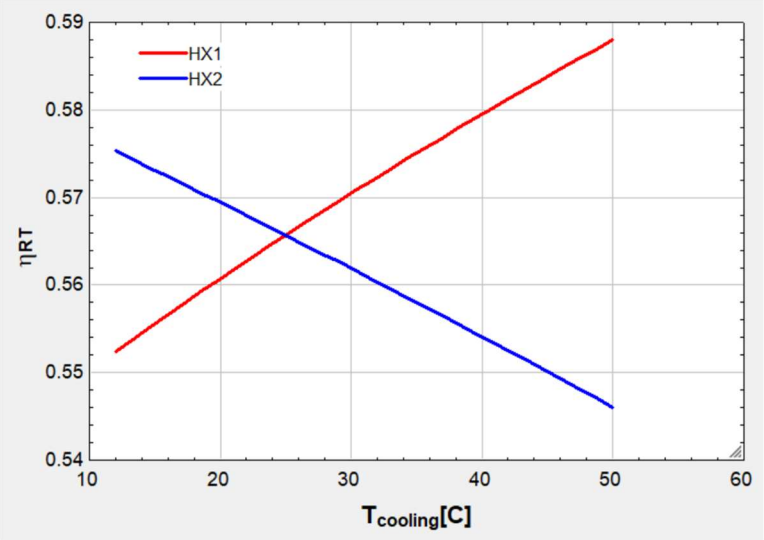

Figure 14. Round-trip efficiency vs. cooling temperature for HX1 and HX2. Plot can be found as Figure 2-2 in the Model 2 Plot windows. All other parameters are their default values.

While the system may theoretically gain a few percent increase in round-trip efficiency, it is important to consider the practicality of changing the cooling fluids to temperatures other than ambient.

HX1 and HX2 effectiveness does not have a significant effect on the round-trip efficiency. Figure 15 demonstrates this by overlaying round-trip efficiency versus effectiveness plots for all four HXs.

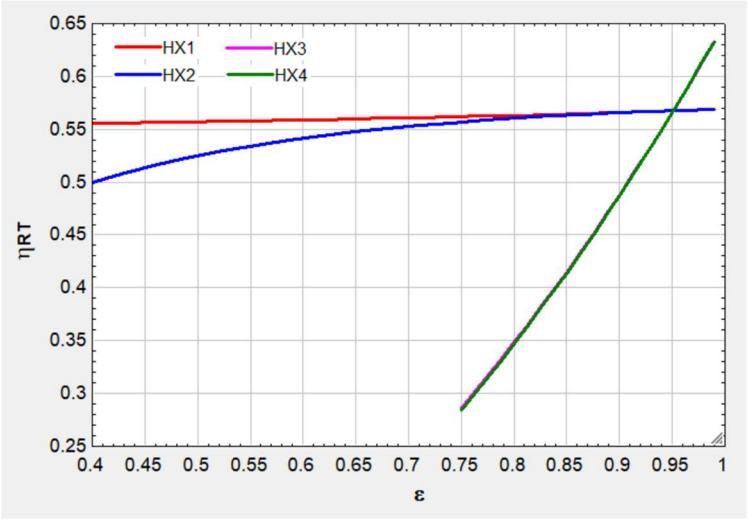

Figure 15. Round-trip efficiency vs. HX effectiveness. Plot can be found as Figure 2-3 in the Model 2 Plot windows. For each plot, just the HX efficiency is modified; all other parameters are their default values. Note that the pink HX3 line is difficult to see as it is closely aligned with the green HX4 line.

HX3 & HX4 effectiveness has a much greater impact on the round-trip efficiency than HX1 & HX2 effectiveness. Additionally, the heat transfer rate between fluids in HX3 & HX4 is much greater than that of HX1 & HX2. For these reasons, HX3 & HX4 will be much larger and more expensive than HX1 & HX2.

Pressure Ratio Effects

Pressure ratio (PR) plays a significant role in the system round-trip efficiency. Figure 16 plots round-trip efficiency versus PR.

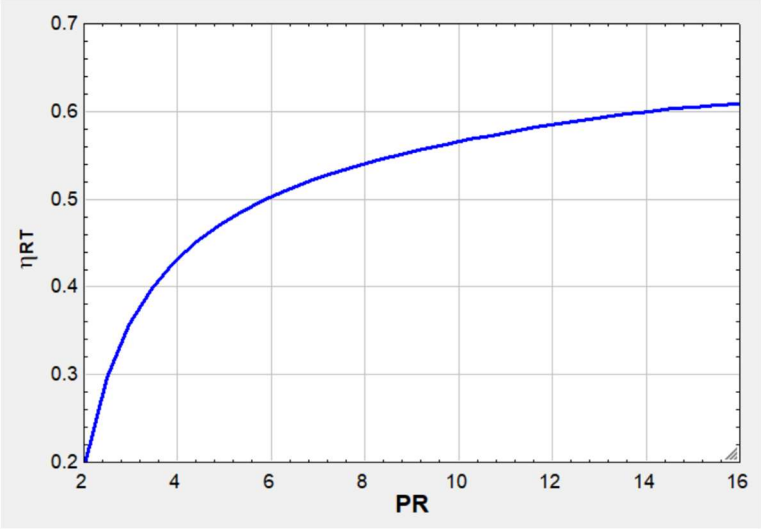

Figure 16. Round-trip efficiency vs. pressure ratio. Plot can be found as Figure 2-4 in the Model 2 Plot windows. All other parameters are their default values.

The trend in Figure 16 is explained by the observations in *System Analysis: Patterns in Round-Trip Efficiency* and Figure 17, which shows two T-s diagrams overlayed for PR values of 5 and 10.

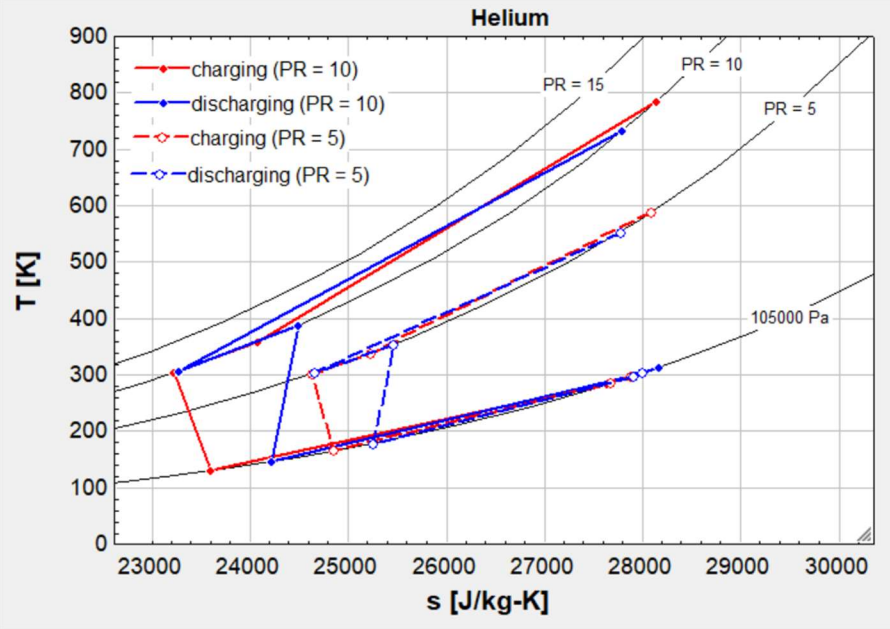

Figure 17. T-s diagrams for PR = 5 and PR = 10. Pressure line at PR = 15 is also shown. Plot can be found as Figure 2-5 in the Model 2 Plot windows. All other parameters are their default values.

It is clear from Figure 17 that as PR increases, so too do the $(h_1 - h_6)$ terms, which benefits round-trip efficiency. Increasing PR also increases the $(h_3 - h_4)$ terms, but the increase is much more significant on the $(h_1 - h_6)$ side. This plot also explains the diminishing returns seen in Figure 16; the temperature difference between PR = 5 and PR = 10 is much greater than the difference between PR = 10 and PR = 15.

Turbomachinery Efficiency Effects

Round-trip efficiency is exceedingly sensitive to changes in turbomachinery efficiency. Figures 18 and 19 show the round-trip efficiency (η_{RT}) versus compressor (η_c) and turbine (η_t) efficiency in a 2D and 3D surface plot, respectively.

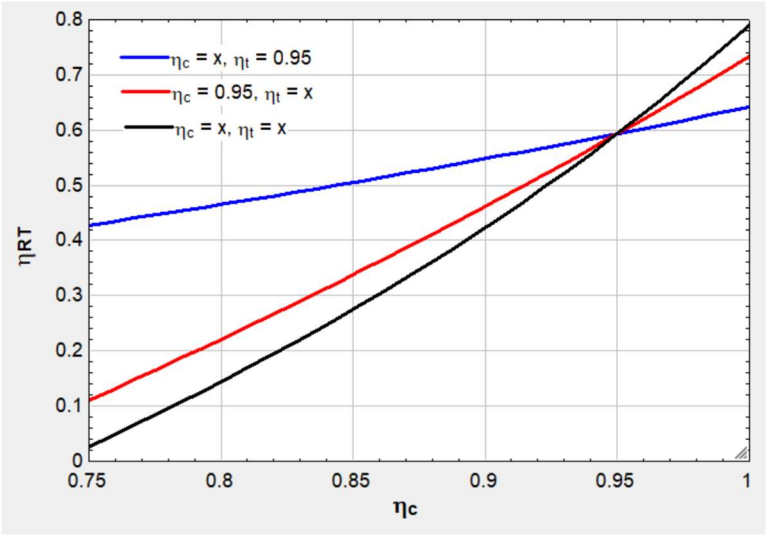

Figure 18. 2D plot of round-trip efficiency (η_{RT}) vs. compressor efficiency (η_c) and turbine efficiency (η_t). Three conditions are shown: (1) η_t is held constant with varying η_c (blue line). (2) η_c is held constant with varying η_t (red line). (3) Both η_c and η_t vary. Plot can be found as Figure 2-7 in the Model 2 Plot windows. All other parameters are their default values.

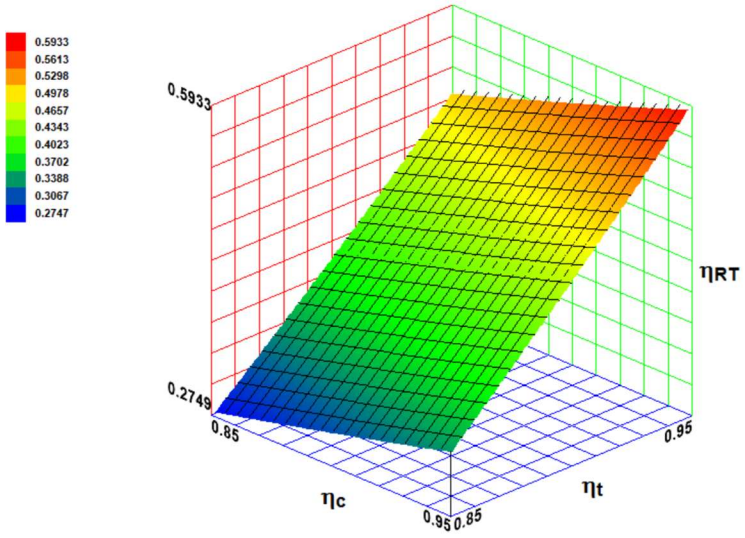

Figure 19. 3D surface plot of round-trip efficiency vs. compressor efficiency (η_c) and turbine efficiency (η_t). Plot can be found as Figure 2-8 in the Model 2 Plot windows. All other parameters are their default values.

It is clear from Figure 18 and Figure 19 that η_t has a greater influence on round-trip efficiency than η_c. This disparity can be explained by examining Equation 9 and the Figure 9 T-s diagram. During the charge phase, HX1 heats the State 5 fluid to State 6, where the fluid is approximately the HX1 water temperature. Because of HX1's influence, the charge State 6 temperature does not change significantly with changing turbomachinery efficiency. Therefore, when the compressor efficiency is increased, charge and discharge State 1 temperature decreases while State 6 remains

approximately the same. Discharge State 6, however, is not directly constrained by HX1; thus, this state significantly reduces temperature with increased turbine efficiency. Additionally, with increased turbine efficiency, discharge State 4 is expanded to a lower temperature, which also pulls discharge State 4 to a lower temperature; this both increases the energy reclaimed by the charging turbine and decreases the energy consumed by the discharging compressor. Figure 20 shows how changes in turbomachinery efficiency persuade the effects described above.

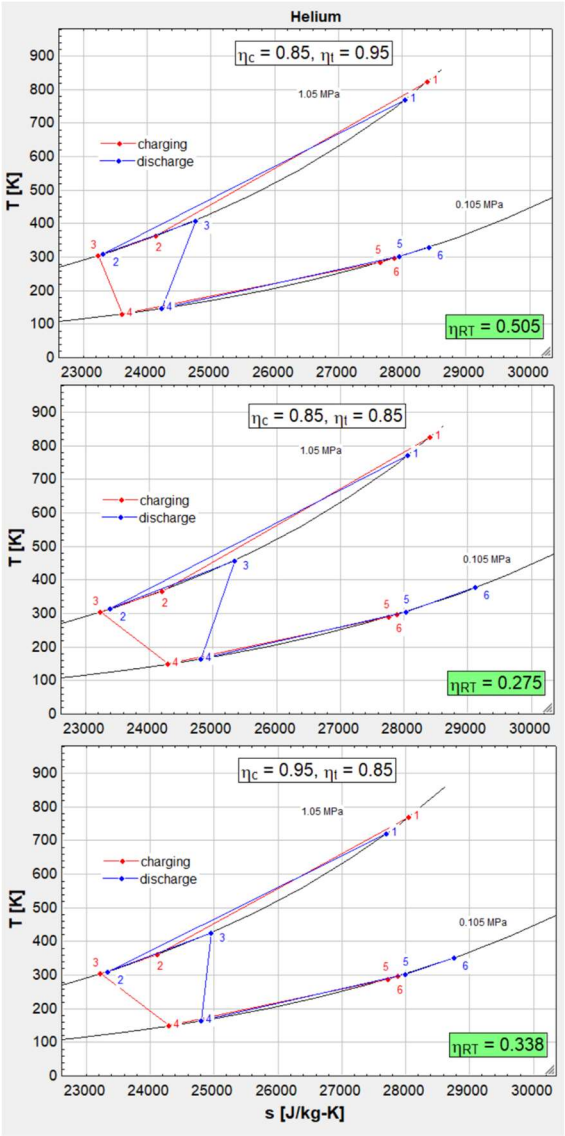

Figure 20. T-s diagrams at three combinations of compressor efficiency and turbine efficiency. Increasing the turbine efficiency provides greater benefits to round-trip efficiency. Plots can be found as Figures 2-9, 2-10, and 2-11 in the Model 2 Plot windows. All other parameters are their default values.

References

[1] H. Ritchie and M. Roser, "Fossil Fuels," *Our World Data*, Nov. 2020, Accessed: Nov. 25, 2021. [Online]. Available: https://ourworldindata.org/fossil-fuels

[2] "How many electric cars are on the road in the United States?," *USAFacts*, Oct. 22, 2020. https://usafacts.org/articles/how-many-electric-cars-in-united-states/ (accessed Nov. 25, 2021).

[3] H. Ritchie and M. Roser, "Electricity Mix," *Our World Data*, Nov. 2020, Accessed: Nov. 26, 2021. [Online]. Available: https://ourworldindata.org/electricity-mix

[4] R. Nunn, J. O'Donnell, J. Shambaugh, L. Goulder, C. Kolstad, and X. Long, "Ten facts about the economics of climate change and climate policy," *Brookings*, Oct. 23, 2019. https://www.brookings.edu/research/ten-facts-about-the-economics-of-climate-change-and-climate-policy/ (accessed Oct. 16, 2021).

[5] D. Rowe, S. Sayeef, and G. Platt, "Chapter 7 - Intermittency: It's the Short-Term That Matters," in *Future of Utilities - Utilities of the Future*, F. P. Sioshansi, Ed. Boston: Academic Press, 2016, pp. 129–150. doi: 10.1016/B978-0-12-804249-6.00007-5.

[6] D. Rowe *et al.*, "Solar intermittency: Australia's clean energy challenge. Characterising the effect of high penetration solar intermittency on Australian electricity networks," 2012, doi: 10.4225/08/584C43986A4C0.

[7] A. Z. AL Shaqsi, K. Sopian, and A. Al-Hinai, "Review of energy storage services, applications, limitations, and benefits," *Energy Rep.*, vol. 6, pp. 288–306, Dec. 2020, doi: 10.1016/j.egyr.2020.07.028.

[8] H. Chen, T. N. Cong, W. Yang, C. Tan, Y. Li, and Y. Ding, "Progress in electrical energy storage system: A critical review," *Prog. Nat. Sci.*, vol. 19, no. 3, pp. 291–312, Mar. 2009, doi: 10.1016/j.pnsc.2008.07.014.

[9] T. M. Gür, "Review of electrical energy storage technologies, materials and systems: challenges and prospects for large-scale grid storage," *Energy Environ. Sci.*, vol. 11, no. 10, pp. 2696–2767, 2018, doi: 10.1039/C8EE01419A.

[10] C. S. Lai and G. Locatelli, "Economic and financial appraisal of novel large-scale energy storage technologies," *Energy*, vol. 214, p. 118954, Jan. 2021, doi: 10.1016/j.energy.2020.118954.

[11] X. Luo, J. Wang, M. Dooner, and J. Clarke, "Overview of current development in electrical energy storage technologies and the application potential in power system operation," *Appl. Energy*, vol. 137, pp. 511–536, Jan. 2015, doi: 10.1016/j.apenergy.2014.09.081.

[12] A. Benato and A. Stoppato, "Pumped Thermal Electricity Storage: A technology overview," *Therm. Sci. Eng. Prog.*, vol. 6, pp. 301–315, Jun. 2018, doi: 10.1016/j.tsep.2018.01.017.

[13] A. J. White, "Loss analysis of thermal reservoirs for electrical energy storage schemes," *Appl. Energy*, vol. 88, no. 11, pp. 4150–4159, Nov. 2011, doi: 10.1016/j.apenergy.2011.04.030.

[14] H. Zhang, L. Wang, X. Lin, and H. Chen, "Technical and economic analysis of Brayton-cycle-based pumped thermal electricity storage systems with direct and indirect thermal energy storage," *Energy*, vol. 239, p. 121966, Jan. 2022, doi: 10.1016/j.energy.2021.121966.

[15] D. Sonar, “Renewable energy based trigeneration systems—technologies, challenges and opportunities,” in *Renewable-Energy-Driven Future*, Elsevier, 2021, pp. 125–168. doi: 10.1016/B978-0-12-820539-6.00004-2.
[16] T. R. Davenne and B. M. Peters, “An Analysis of Pumped Thermal Energy Storage With De-coupled Thermal Stores,” *Front. Energy Res.*, vol. 8, p. 160, Aug. 2020, doi: 10.3389/fenrg.2020.00160.
[17] “Team connects first grid-scale pumped heat energy storage system,” *The Engineer*, Jan. 09, 2019. https://www.theengineer.co.uk/grid-scale-pumped-heat-energy-storage/ (accessed Nov. 20, 2021).
[18] “Ground-breaking energy storage operational in Newcastle,” *https://networks.online/*, Jan. 11, 2019. https://networks.online/gas/ground-breaking-energy-storage-operational-in-newcastle/ (accessed Nov. 20, 2021).
[19] J. D. McTigue, A. J. White, and C. N. Markides, “Parametric studies and optimisation of pumped thermal electricity storage,” *Appl. Energy*, vol. 137, pp. 800–811, Jan. 2015, doi: 10.1016/j.apenergy.2014.08.039.
[20] “Diagram Window,” *F-Chart Software*. https://fchart.com/ees/eeshelp/1phh4av.htm (accessed Dec. 18, 2021).
[21] Engineering Equation Solver, *The Diagram Window in EES*, (Oct. 21, 2016). Accessed: Dec. 18, 2021. [Online Video]. Available: https://www.youtube.com/watch?v=nyLPOAEYTOs